Phylogenomic datasets provide both precision and accuracy in estimating the timescale of placental mammal phylogeny

Mario dos Reis[1], Jun Inoue[1,2], Masami Hasegawa[3], Robert J. Asher[4], Philip C. J. Donoghue[5],* and Ziheng Yang*,[1]

[1]*Department of Genetics, Evolution and Environment, University College London, Darwin Building, Gower Street, London, UK*
[2]*Atmosphere and Ocean Research Institute, University of Tokyo, Kashiwa, Chiba, Japan*
[3]*School of Life Sciences, Fudan University, Handan Road no. 220, Shangai 200433, China*
[4]*Museum of Zoology, University of Cambridge, Downing Street, Cambridge, UK*
[5]*School of Earth Sciences, University of Bristol, Wills Memorial Building, Queen's Road, Bristol, UK*

The fossil record suggests a rapid radiation of placental mammals following the Cretaceous–Paleogene (K–Pg) mass extinction 65 million years ago (Ma); nevertheless, molecular time estimates, while highly variable, are generally much older. Early molecular studies suffer from inadequate dating methods, reliance on the molecular clock, and simplistic and over-confident interpretations of the fossil record. More recent studies have used Bayesian dating methods that circumvent those issues, but the use of limited data has led to large estimation uncertainties, precluding a decisive conclusion on the timing of mammalian diversifications. Here we use a powerful Bayesian method to analyse 36 nuclear genomes and 274 mitochondrial genomes (20.6 million base pairs), combined with robust but flexible fossil calibrations. Our posterior time estimates suggest that marsupials diverged from eutherians 168–178 Ma, and crown Marsupialia diverged 64–84 Ma. Placentalia diverged 88–90 Ma, and present-day placental orders (except Primates and Xenarthra) originated in a ~20 Myr window (45–65 Ma) after the K–Pg extinction. Therefore we reject a pre K–Pg model of placental ordinal diversification. We suggest other infamous instances of mismatch between molecular and palaeontological divergence time estimates will be resolved with this same approach.

Keywords: divergence time; fossil; mammal; Bayesian analysis

1. INTRODUCTION

Controversy over the timing of placental mammal diversification relative to the Cretaceous–Paleogene, (K–Pg) mass extinction event ignited debate over the veracity of palaeontological versus molecular approaches to divergence time estimation [1]. Fossil representatives of crown placental orders appear in the 16 Myr (million years) interval following the K–Pg extinction [2], indicating a diversification peak between 65 and 60 Ma (millions of years ago) [3], and consistent with a Paleogene radiation of placentals after the sudden disappearance of non-avian dinosaurs and other species during the mass extinction event [4]. Early molecular studies (most notably [5], see also [6]) found ancient dates of origination of placental mammals, pre-dating the K–Pg extinction. Although it is expected that the earliest fossil evidence for a divergence will postdate the event itself, the time lag between these molecular time estimates and the placental mammal fossil record has been considered unacceptably large [7,8].

Archibald & Deutschman [2] proposed three models of placental mammal diversification with respect to the K–Pg event and their relationship to the fossil record. In the explosive model, the last common ancestor of Placentalia originated and diversified in the Paleogene. In the long-fuse model, the ancestor of Placentalia originated in the Cretaceous but intraordinal diversification (the evolution of new families and genera within orders) occurred in the Paleogene, agreeing with fossil finds of modern orders postdating the K–Pg event, but acknowledging an ancient origin for Placentalia. Finally, in the short fuse model, several placental orders diversified in the Cretaceous shortly after the origination of Placentalia, with the others diversifying in the Paleogene. This last model implies that Middle- and even Early Cretaceous crown placental mammals existed, but have not yet been recovered from an otherwise diverse mammalian fossil record. Palaeontological interpretations of crown placental lineages deep within the Cretaceous [9,10] have been contested on phylogenetic and anatomical grounds [11–13].

Nevertheless, the fossil record provides only a minimum estimate for the antiquity of a given clade, and molecular clock studies contradict the explosive model of a Paleogene origin for Placentalia. Some of these studies date the origin of Placentalia at more than 100 Ma, deep within the Cretaceous [5,14–17]. Others indicate a younger (*ca* 80–90 Ma) Cretaceous last common ancestor for Placentalia [18,19]. Although molecular studies have

* Authors for correspondence (phil.donoghue@bristol.ac.uk; z.yang@ucl.ac.uk).

agreed on a Cretaceous origin for Placentalia, they disagree on the extent of ordinal level diversification relative to the K–Pg event. For example, a supertree-based molecular study of over 4000 mammal taxa by Bininda-Emonds *et al.* [16] found that half of the placental orders originated deep in the Cretaceous, much earlier than any known fossil record of those groups. However, this study employed a heuristic time estimation method that does not account appropriately for lineage rate variation, used a point fossil calibration for the mammalian root, and did not account for uncertainty in branch length estimation. More recently, Meredith *et al.* [17] used a supermatrix of 164 taxa and 26 genes, and found younger dates of intraordinal diversification, with five placental orders presenting large credibility intervals extending from the Early Cretaceous to the Late Paleocene. However, the limited statistical power afforded by the small sequence dataset resulted in error margins on divergence time estimates that are too broad to determine whether placental diversification occurred mainly in the Cretaceous or in the Paleocene (i.e. short versus long fuse models).

Here we take advantage of the whole genome sequence data now available for tens of mammal species [20], together with multiple, fossil-based temporal constraints encompassing the breadth of mammalian phylogeny [21], to establish a refined timescale for the placental mammal evolution. We use a Bayesian approach that integrates over the uncertainty in rate variation along the phylogeny and facilitates analysis of very large alignments [22–24]. In a Bayesian analysis, fossil constraints impose a theoretical limit on the precision of posterior time estimates [22,25]. We set out to determine whether current genome scale data are enough to approach this theoretical limit, and whether the precision achievable in divergence time estimation is sufficient to confidently reject the hypothesis of post K–Pg diversification of placental mammal orders.

2. METHODS

Our analysis was performed in two stages. First, we performed Bayesian estimation of divergence times on a set of 14 632 nuclear gene alignments (20.6×10^6 base pairs) for 36 mammalian species (33 placentals, two marsupials and one monotreme). In the second stage, the posterior probability of divergence times obtained in the first stage was used to construct the time prior for an analysis of the 12 protein genes encoded on the heavy strand of the mitochondrial genome of 274 mammal species, and Bayesian estimation of divergence times proceeded on this dataset. The result is effectively a combined analysis of nuclear and mitochondrial genomes.

(a) *Taxon sampling, molecular data and tree topology*
Confirmed and predicted copy DNA (cDNA) sequences for the 36 mammalian genomes were downloaded from Ensembl v. 56. The Ensembl database provides detailed information about orthology and paralogy for the mammalian genome [20]. A rooted tree was constructed based on the literature [26,27]. The tree and species list are presented in figure 1. Only gene sequences identified as one-to-one orthologues between human and the remaining 35 species were analysed, and only the longest splicing variant for each cDNA sequence was considered. The mitochondrial genome sequences from 274 mammal species were downloaded from GenBank. The

list of 274 mammal species and their tree topology are given in the electronic supplementary material, figure S1.

Amino acid sequences for the nuclear genomes were aligned using PRANK [28] according to the rooted guide tree. The following gene alignments were discarded: genes that did not have a mouse orthologue, genes for which sequences could be found for fewer than 10 of the 36 species and genes shorter than 100 codons. Furthermore, for each gene alignment, a phylogentic tree was estimated by maximum likelihood (ML) using RAxML v. 7.2.1 [29]. Alignments where at least one sequence was associated with an unusually long external branch (that accounted for more than 60% of total tree length) were also removed. This left a dataset of 14 632 nuclear gene alignments. The amino acid sequences were reverse translated to generate DNA alignments. For the mitochondrial genomes, only the 12 protein genes encoded on the heavy strand were analysed. Amino acid and DNA alignments were generated as for the nuclear gene dataset. The tree topology for the 274 species was estimated with RAxML using the 36 species tree as a guide tree. Well-supported marsupial, bovid, carnivoran, pholidote, euarchontan and chiropteran clades identified from the literature were fixed into the guide tree [26,30–34].

The 14 632 nuclear gene alignments were divided into 20 partitions based on the relative substitution rate, with about the same number of genes in each partition. Because the number of species within each alignment varies from 10 to 36, we measured the relative rate by the *p*-distance between amino acid sequences of human and mouse. The 12 protein genes in the mitochondrial alignment of 278 species were treated as a single partition. Third codon positions in both the nuclear and mitochondrial alignments were excluded from all dating analyses.

(b) *Bayesian divergence time estimation*
The analysis of divergence times was conducted using the program MCMCTree v. 4.4e [35]. Exact calculation of the likelihood function during Markov chain Monte Carlo (MCMC) iteration is computationally expensive, and so we used the approximate method [24,36]. First we calculated the maximum-likelihood estimates of the branch lengths, the gradient vector and Hessian matrix, using the BaseML and CodeML programs [35]. We used branch-by-branch optimization, as it provided quick convergence for the large datasets. We used the HKY + Γ_4 model [37,38] for the DNA datasets, the WAG + F + Γ_4 model [39] for the nuclear encoded proteins and the MTMAM + F + Γ_4 model [40] for the mitochondrial proteins. The second step uses an MCMC algorithm to estimate divergence times on the tree topology. The gradient vector and Hessian matrix are used to generate the Taylor expansion of the log-likelihood. This approximation saves much computation time during the MCMC on large alignments.

The auto-correlated rates model [22,36] was used to specify the prior of rates. The time unit was 100 Myr. We used a diffuse gamma prior G(1, 1) for the overall substitution rate, with mean 1, meaning 10^{-8} changes per site per year. The rate drift parameter σ^2 was assigned G(1, 1). Parameter σ^2 reflects the amount of rate variation across lineages or how seriously the molecular clock is violated. The parameters of the birth–death process with species sampling were fixed at $\lambda = \mu = 1$ and $\rho = 0$. We tested a series of informative priors on the overall rate based on rough rate estimates obtained by fitting a molecular clock
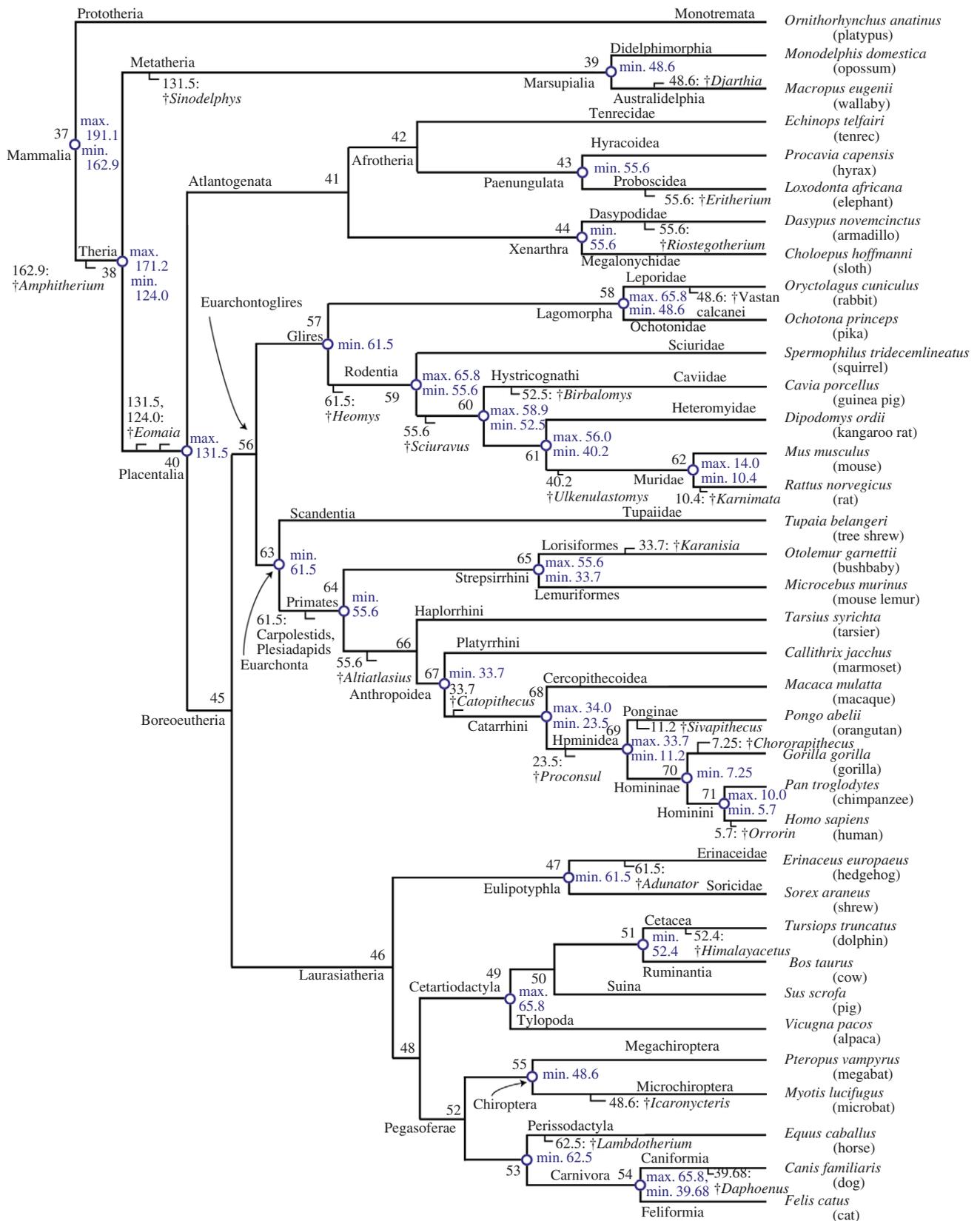
Figure 1. The tree of 36 mammal species showing fossil calibrations. Calibration bounds are soft; that is, the probability that the true divergence time is outside the bounds is small but non-zero. Internal nodes are numbered from 37 to 71. The tree topology follows the literature [26,27]. The 'dagger' symbol shows a species which is extinct.

to the sequence data using point calibrations. However, these priors did not affect estimated posterior times noticeably, possibly because the fossil calibrations, which occur throughout the phylogeny, constrain the time prior. The number of iterations, the burn-in and the sampling frequency were determined in test runs of the program. Every analysis was conducted at least twice to ensure convergence of the MCMC.

(c) *Fossil calibrations and time prior*

We used 26 fossil calibrations on the 36 species tree: 12 joint (maximum and minimum), two maximum and 12 minimum bounds (figure 1 and electronic supplementary material, table S1). Both minimum and maximum bounds were 'soft', that is we set the probability that the true divergence time is outside the bounds to be small, but non-zero, allowing molecular data to correct for conflicting fossil information [25]. Minimum bounds are represented using truncated Cauchy distributions [41] with a left tail probability of 0.1 per cent. For maximum and joint bounds, the default 2.5 per cent tail probability was used. MCMC runs were carried out without using the sequences to estimate the time prior and to check for consistency with the fossil calibrations.

The marginal posterior of divergence times obtained from the 14 632 nuclear gene dataset was used to construct the time prior for the 274 species mitochondrial gene dataset. A Skew-t distribution was fitted by ML to each posterior node age in the 35 species tree (sm package, R), and used as calibrations for the appropriate nodes in the 274 species tree. The Skew-t distribution is very flexible, and can approximate a range of unimodal distributions with arbitrary skewness and kurtosis. This effectively results in a combined analysis of nuclear and mitochondrial genes to estimate divergence times. A simultaneous multi-partition analysis, with the mitochondrial proteins in one partition, and the 14 632 nuclear genes arranged in several partitions, would have been the ideal way to estimate divergence times for all 274 species. However, such an analysis would have been computationally expensive (many months) with the current MCMCTREE implementation.

(d) *Data partitioning*

A total of 857 of the nuclear genes are present in all 36 mammalian genomes. We used this data subset for several exploratory analyses and so we analysed these genes in a single partition as an amino acid alignment and as a nucleotide alignment. We then explored two partitioning strategies. In the first, we divided the 857 genes into 10 or 20 partitions with approximately the same number of genes according to their relative substitution rate, measured by the tree length (sum of branch lengths) on the tree of figure 1. Branch lengths for each gene were estimated with RAxML using the GTR + Γ model.

In the second strategy, we used principal component analysis (PCA) on the branch lengths, and k-means clustering on the PCA components to generate the partitions. For each nucleotide alignment of first and second codon positions, the branch lengths were estimated by ML with RAxML using the GTR + Γ substitution model on the fixed tree. We constructed a matrix of absolute branch lengths, $\mathbf{B} = (b_{ij})$, with 857 rows and $2 \times 36 - 3 = 69$ columns (trees are unrooted), and a matrix of relative branch lengths, $\mathbf{R} = (r_{ij})$ where $r_{ij} = b_{ij}/\sum_j b_{ij}$. Four transformed matrices were constructed $\mathbf{L} = (\log\ b_{ij})$, $\mathbf{S} = (\sqrt{b_{ij}})$, $\mathbf{L}_r = (\log r_{ij})$ and $\mathbf{S}_r = (\sqrt{r_{ij}})$. On each one of the four transformed matrices, a PCA was performed to try to identify patterns in branch length variation across orthologues. The first principal component in the analyses using absolute branch lengths was highly correlated with total tree length. A robust version of the k-means clustering algorithm (PAM [42]) was used to group the 857 alignments into 10 partitions using the first two axes of the PCA.

3. RESULTS AND DISCUSSION

Our results are summarized in figure 2a and table 1. Detailed time estimates for the divergences in the 274-species tree are given in the electronic supplementary material, figure S1. We estimated the origin of placentals at 88–90 Ma, substantially younger than some previous estimates [5,14–16], but congruent with others [17–19]. With the exception of Xenarthra and Primates, placental orders diversified in the 20 Myr interval following the K–Pg extinction event. For example, within Laurasiatheria, the ancestral lineages of cats, dogs, bears, bats, horses, rhinoceros, whales, ruminants, pigs, camels, hedgehogs, moles and shrews are estimated to have originated by 45 Ma. However, the divergences of each of their crown parent clades (Cetartiodactyla, Carnivora, Chiroptera and Eulipotyphla) did not occur until after 62 Ma (figure 2a and the electronic supplementary material, figure S1). Similarly, diversification of the crown clades within Afrotheria, Euarchontoglires (except Primates) and even Marsupialia are estimated to have occurred soon after the K–Pg extinction event, with the establishment of morphologically diverse lineages within approximately 20 Myr (figure 2a and the electronic supplementary material, figure S1). Crown Primates and crown Xenarthra are estimated to have diverged just before the K–Pg event, at 69–67 Ma and 72–67 Ma, respectively, with the fundamental splits within these groups occurring well within the Paleogene (electronic supplementary material, figure S1).

Bininda-Emonds *et al.* [16] dated the age of 9 of 18 crown placental orders to be before the K–Pg event. They proposed a delayed rise model of placental diversification to explain the large time gap between the origination of crown orders in the Cretaceous and their lineage diversification in the Paleogene. For example, they dated crown Chiroptera at 74.9 Ma, Primates at 87.7 Ma, Lagomorpha at 66.8 Ma and Rodentia at 85.3 Ma, while there are no Cretaceous fossil representatives for these groups [7]. Our estimates suggest a post K–Pg origination for ordinal level crown groups, consistent with the fossil record. For comparison, we date Chiroptera at 59.1 Ma, Primates at 68.2 Ma, Lagomorpha at 47.9 Ma and Rodentia at 64.4 Ma. We conclude that there is no evidence to support a delayed rise model.

Our large genome scale alignment is very informative, contributing to a concentrated posterior time distribution for almost all ordinal placental divergences (table 1 and figure 3). Our credibility intervals are much narrower than those reported in other studies ([17], electronic supplementary material, figure S2), even though the time prior is rather diffuse, encompassing both pre and post-K–Pg divergences for many ordinal level crown groups (table 1). Construction of the time prior is a complex process as it accounts for the fossil age constraints, the birth–death process and the age constraints required by the hierarchical ordering of nodes in the tree (electronic supplementary material, text). In particular, the marginal prior of a node may differ from its fossil calibration [43]. We note the importance of estimating the time prior explicitly so that it can be compared with the time posterior and the fossil calibrations (figure 3).

The use of soft calibration densities allows the data to correct for conflicting fossil-based time constraints. For example, the estimated age of crown Theria (node 38),
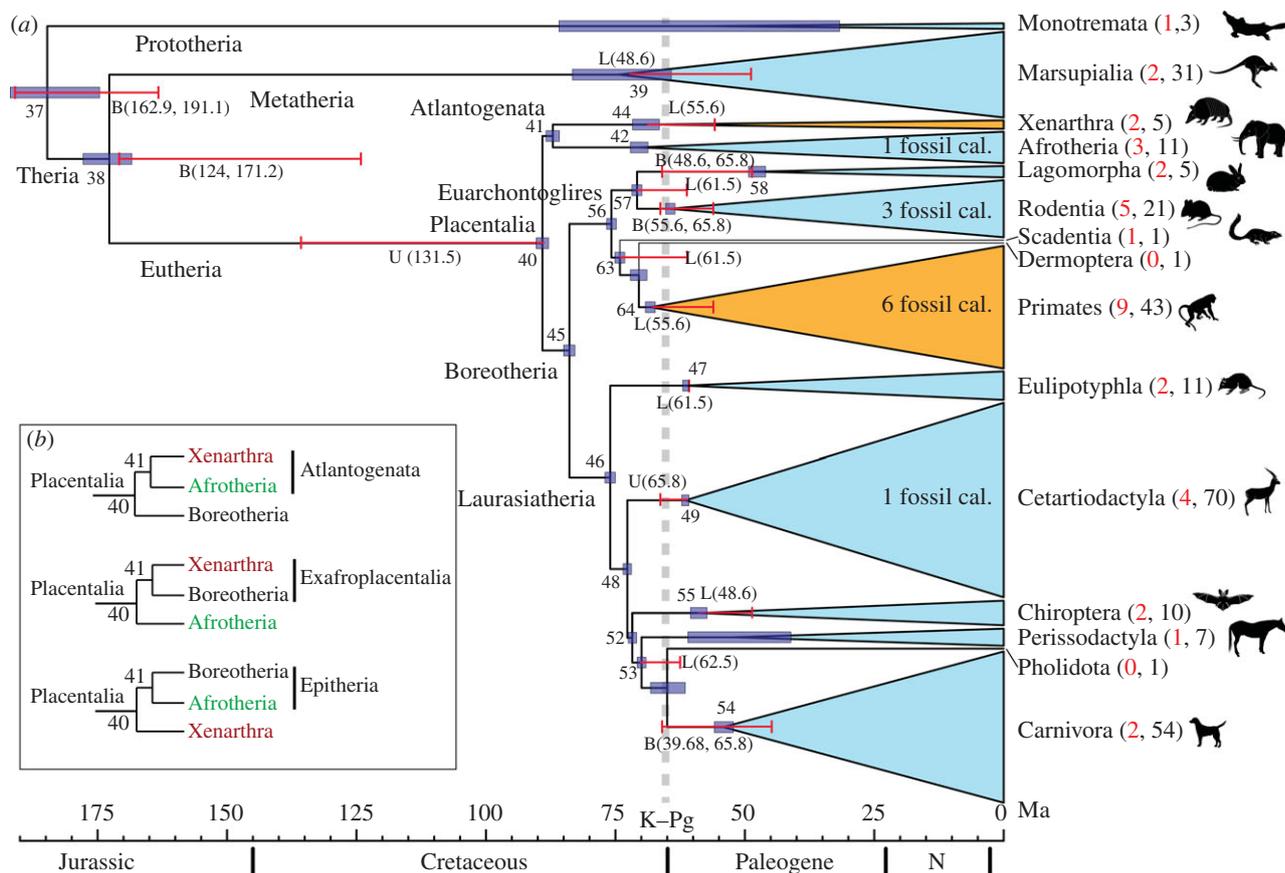
Figure 2. The timetree of mammals. (*a*) Blue horizontal bars represent the posterior 95% CI for the node ages. Red horizontal bars represent fossil calibrations: U for upper (maximum), L for lower (minimum) and B for both. The number of species analysed is presented within brackets: red for nuclear and black for mitochondrial genomes. The two mammal orders that diversified before the K–Pg event are shown in orange. All orders within Afrotheria and Marsupialia diversified after the K–Pg event. The tree topology follows [26,27]. (*b*) The three possible topologies concerning the divergence of early Placentalia.

178–168 Ma, violates our fossil-based soft maximum age constraint for this node (figure 3 and table 1). However, our posterior estimate is in accord with a recently described eutherian fossil dated approximately 153 Ma [44] (electronic supplementary material, figure S3). This highlights the robustness of soft fossil-based age constraints and large informative sequence datasets to palaeontological uncertainty. The posterior ages of nodes 58 (lagomorphs) and 60 (guinea pig/rat) also violated their corresponding fossil calibrations (figure 3). To assess the robustness of our estimated times to the presence of these problematic calibrations [45], we performed an additional analysis on the 36 species tree where we removed the maximum age constraints on nodes 38 (crown Theria) and 60 (guinea pig/rat), and the joint constraints on lagomorphs (node 58). We found that the estimated age of crown Theria became older (the posterior mean and credibility interval (CI) changed from 175, 170–182 Ma to 186, 181–191 Ma), while the guinea pig/rat clade (node 60) became younger (the posterior mean and CI changed from 47.8, 45.8–49.3 Ma to 45.6, 42.9–48.2 Ma). The ages of all other nodes (including guinea pig/rat; node 60) were only marginally affected (electronic supplementary material, figure S4). Thus our estimated times are robust to the presence of this conflicting fossil evidence for calibrations.

We tested whether current genomic data are sufficient to reduce uncertainty in time estimates towards its theoretical limit. With a relaxed clock, as the number of sites and loci approach infinity, a scatter plot of posterior mean times (divergence) versus their corresponding CI widths (uncertainty) approaches a straight line [22]. Figure 4*a* shows the scatter plot for the time prior, showing the high level of uncertainty owing to the soft fossil constraints: for every 100 Myr of divergence, 47 Myr of uncertainty is added to the prior CI width. For the time posterior calculated using 36 species and 14 632 genes, the scatter plot is close to a straight line (figure 4*b*). The addition of molecular data reduces uncertainty substantially, and for every 100 Myr of divergence, only 6.4 Myr of uncertainty is added to the posterior CI width (figure 4*b*). Marsupialia (node 39) is a clear outlier, exhibiting much greater uncertainty than expected, given the age of the clade. Increased taxon sampling through the inclusion of the mitochondrial data reduced substantially the uncertainty on the age of Marsupialia (figure 4*c*). Our analysis indicates that current genome scale sequence data yield results close to the theoretical limit of uncertainty for the ages of mammalian ordinal and supraordinal clades. However, the uncertainty associated with divergences at family and genus levels is high (grey points in figure 4*c*), and increased density of taxon-sampling at genome scale will probably improve their age estimates substantially.

Extensive tests indicate that our divergence time estimates are robust to the substitution model (protein

Table 1. Prior and posterior divergence times for selected nodes in the mammal tree.

	node	marginal prior[a,d]	combined, 14 K + Mit[b,d]	14 K, Atlantogenata[c,d]	14 K, Epitheria[c,d]	14 K, Exafroplacentalia[c,d]
37	root	177.7 (163.1, 191.2)	184.6 (174.1, 191.9)	185.0 (174.5, 191.8)	188.8 (182.5, 192.6)	184.1 (173.1, 191.7)
38	Theria	149.4 (125.7, 170.9)	172.8 (168.4, 177.8)	175.4 (170.4, 181.7)	184.9 (178.1, 190.4)	173.4 (169.0, 179.2)
39	Marsupialia	90.6 (50.8, 139.4)	75.1 (64.4, 84.0)	66.7 (50.7, 83.7)	64.9 (50.3, 86.0)	67.7 (51.4, 83.4)
40	Placentalia	124.1 (102.1, 139.2)	89.1 (87.9, 90.4)	89.9 (88.3, 91.6)	92.2 (90.4, 93.8)	92.2 (90.6, 93.8)
41	*[e]	113.3 (77.9, 134.4)	87.1 (85.8, 88.4)	87.5 (85.9, 89.1)	90.5 (88.8, 92.1)	90.2 (88.7, 91.7)
42	Afrotheria	95.1 (59.9, 129.2)	70.4 (68.7, 72.1)	70.4 (68.5, 72.4)	71.1 (69.1, 73.3)	73.1 (71.1, 74.8)
43	Paenungulata	75.9 (56.1, 117.3)	60.3 (58.4, 62.2)	59.8 (57.7, 61.8)	61.8 (59.7, 64.1)	64.5 (62.4, 66.2)
44	Xenarthra	86.5 (56.9, 126.0)	69.4 (66.5, 71.8)	70.0 (67.3, 72.4)	75.4 (72.3, 77.3)	72.7 (70.7, 74.8)
45	Boreotheria	120.5 (97.8, 136.6)	83.8 (82.8, 84.9)	82.4 (81.1, 83.8)	82.1 (80.7, 83.5)	82.7 (81.4, 84.0)
46	Laurasiatheria	114.6 (87.0, 133.9)	76.0 (74.9, 77.0)	76.0 (74.8, 77.1)	75.6 (74.4, 76.7)	75.7 (74.6, 76.8)
47	Eulipotyphla	91.7 (62.9, 126.4)	61.5 (60.9, 62.0)	61.3 (60.6, 61.8)	61.4 (60.6, 61.9)	61.5 (61.0, 62.1)
48	cow/horse	105.7 (74.1, 130.8)	72.7 (71.9, 73.6)	73.1 (72.0, 74.2)	72.8 (71.7, 73.8)	73.1 (72.1, 74.1)
49	Cetartiodactyla	63.6 (55.8, 70.4)	61.4 (60.8, 62.3)	61.4 (60.7, 62.3)	61.2 (60.5, 61.9)	61.1 (60.5, 61.8)
50	pig/cow	60.0 (53.4, 67.4)	58.1 (57.5, 58.9)	58.0 (57.4, 58.8)	57.8 (57.3, 58.5)	57.8 (57.3, 58.5)
51	dolphin/cow	56.6 (52.5, 64.5)	52.8 (52.3, 53.9)	52.7 (52.2, 53.7)	52.6 (52.2, 53.4)	52.5 (52.1, 53.2)
52	horse/cat/bat	96.0 (66.4, 126.7)	71.7 (70.8, 72.5)	72.2 (71.2, 73.3)	71.9 (70.9, 72.9)	72.1 (71.2, 73.2)
53	horse/cat	80.6 (63.0, 115.4)	69.9 (69.1, 70.8)	70.1 (69.1, 71.1)	69.8 (68.8, 70.8)	70.1 (69.2, 71.1)
54	Carnivora	53.2 (39.7, 65.7)	54.2 (52.3, 56.0)	54.1 (52.0, 55.9)	53.6 (51.6, 55.4)	52.9 (50.7, 54.9)
55	Chiroptera	71.1 (49.6, 111.0)	59.1 (57.7, 60.6)	59.3 (57.6, 60.8)	59.4 (57.9, 60.9)	60.3 (58.8, 61.7)
56	Euarchontoglires	114.0 (87.4, 133.3)	75.8 (74.9, 76.7)	75.8 (74.6, 77.0)	75.4 (74.2, 76.6)	75.5 (74.3, 76.6)
57	Glires	90.8 (64.0, 125.2)	70.8 (69.9, 71.8)	70.7 (69.6, 71.8)	70.5 (69.4, 71.6)	70.8 (69.7, 71.8)
58	Lagomorpha	57.5 (48.6, 65.8)	47.9 (46.0, 49.3)	47.8 (45.8, 49.3)	47.5 (45.4, 49.1)	46.7 (44.4, 48.6)
59	Rodentia	61.1 (56.0, 65.8)	64.4 (63.5, 65.3)	64.5 (63.4, 65.5)	64.2 (63.1, 65.2)	64.2 (63.1, 65.2)
60	guinea pig/rat	55.8 (52.5, 58.9)	61.3 (60.5, 62.2)	61.3 (60.3, 62.2)	61.1 (60.0, 62.0)	61.1 (60.1, 62.1)
61	kangaroo rat/rat	47.7 (40.2, 55.6)	56.0 (55.1, 56.8)	55.6 (54.4, 56.5)	55.3 (54.1, 56.3)	55.1 (53.9, 56.2)
62	mouse/rat	12.2 (10.4, 14.0)	14.0 (13.5, 14.4)	13.9 (13.2, 14.3)	13.9 (13.2, 14.3)	13.9 (13.4, 14.4)
63	Euarchonta	100.8 (69.4, 128.8)	74.1 (73.2, 75.1)	74.2 (73.0, 75.3)	73.8 (72.6, 75.0)	74.0 (72.9, 75.1)
64	Primates	81.9 (57.7, 115.1)	68.2 (67.3, 69.1)	69.0 (67.8, 70.1)	68.6 (67.4, 69.7)	68.4 (67.3, 69.5)
65	Strepsirrhini	44.9 (33.7, 55.7)	55.1 (53.4, 56.8)	54.3 (52.3, 55.8)	54.4 (52.5, 55.9)	54.9 (53.2, 56.2)
66	human/tarsier	64.1 (42.5, 99.5)	65.0 (64.0, 65.9)	65.0 (63.9, 66.0)	64.7 (63.6, 65.8)	64.7 (63.6, 65.7)
67	Anthropoidea	48.2 (34.3, 76.4)	37.4 (35.9, 39.0)	36.6 (34.9, 38.3)	36.1 (34.5, 37.7)	35.6 (34.1, 37.3)
68	Catarrhini	29.5 (23.7, 34.1)	26.4 (25.3, 27.4)	25.6 (24.4, 26.8)	25.3 (24.2, 26.5)	25.0 (24.0, 26.3)
69	human/orang	21.5 (11.7, 31.6)	17.1 (16.2, 18.1)	17.3 (16.2, 18.4)	17.1 (16.1, 18.1)	16.8 (15.8, 17.9)
70	human/gorilla	12.8 (7.7, 23.2)	10.4 (9.8, 11.0)	10.2 (9.6, 11.0)	10.1 (9.5, 10.8)	9.9 (9.3, 10.6)
71	human/chimpanzee	7.7 (5.7, 10.0)	8.2 (7.6, 8.8)	8.7 (8.1, 9.4)	8.5 (8.0, 9.2)	8.4 (7.8, 9.0)

[a] The marginal prior of a node is constructed from the fossil calibrations or from a birth–death process for nodes with no fossil calibration.
[b] Posterior time estimate for the combined analysis of 14 K nuclear genes and mitochondrial data for 274 species.
[c] Posterior time estimates for 14 K nuclear genes for 36 species, assuming each of the three different basal Placentalia topologies (figure 2b).
[d] Values are mean and 95% CI (in brackets). Clade ages are the ages of the corresponding crown groups.
[e] Node 41 represents basal Atlantogenata, Epitheria or Exafroplacentalia, according to the placental topology considered (figure 2b). Node numbers correspond with those in figure 1.
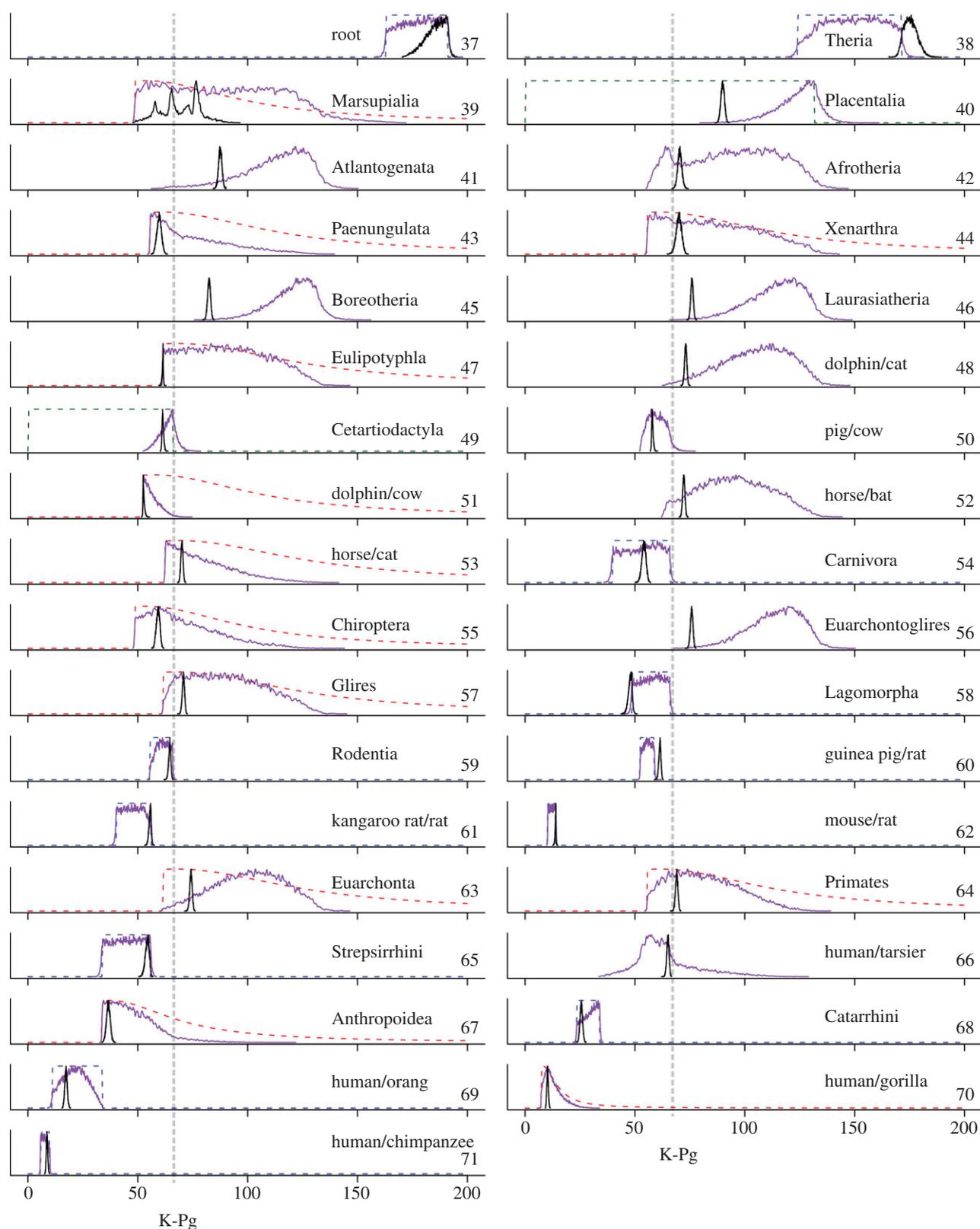
Figure 3. Calibrations, prior and posterior densities. The marginal posterior density of divergence times estimated from the 14 346 nuclear genes is shown in black. The marginal prior density of times is shown in purple. The fossil calibrations are shown as dashed lines in red (minimum bound), green (maximum bound) and blue (joint). Nodes with no calibrations (41, 42, 45, 46, 48, 50, 52, 56 and 66) have their marginal priors generated using the birth–death process conditioned on the ages of the calibration nodes [25] (see the electronic supplementary material, text). Note how the marginal prior densities may differ from the corresponding fossil calibration densities. All densities are scaled so that their maximum is one. Time scale is in million years ago. Clade ages are the ages of the corresponding crown groups.

versus nucleotide), to variations in the number of genes and gene partitions, and to various partitioning strategies based on multivariate analysis and clustering of branch

lengths (electronic supplementary material, figure S5). In particular, sophisticated partitioning strategies based on PCA did not perform better than the simpler rate-
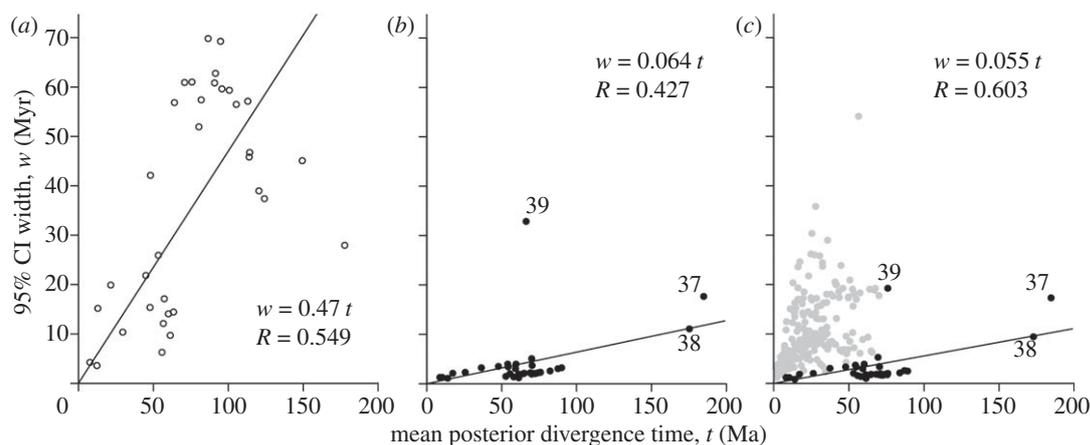
Figure 4. Infinite-sites plot. The 95% CI width is plotted against the mean of the divergence time. (*a*) Prior calculated from a MCMC without sequence data on the 36-species tree. (*b*) Posterior calculated using 14 632 nuclear genes in 20 partitions, 36 species. (*c*) Posterior from combined analysis of 14 632 nuclear genes in 20 partitions and 12 mitochondrial genes for 274 species in one partition. In (*c*), black dots indicate nodes shared with the 36-species tree, and grey dots indicate nodes that are exclusive to the 274-species tree. Only black dots are used to fit the line and calculate R.

based partition strategy. Our results are also robust to tree topology. The three main groups of placental mammals (Boreotheria, Xenarthra and Afrotheria) diverged almost simultaneously [27] and there is uncertainty regarding the position of the placental root [27,46]. Our principal analyses assumed the Atlantogenata hypothesis of placental divergence (figure 2*b*). Estimated divergence times using the two alternative Placentalia trees (figure 2*b*) yield very similar clade ages (table 1), indicating that our divergence time estimates are robust to these topological differences. The three superorders are thought to reflect the radiation of early placentals among the three principal continental land masses resulting from the break-up of Pangaea: Boreotheria in North America, Asia and Europe; Xenarthra in South America; and Afrotheria in Africa [26,27,47]. However, our age estimate for crown Placentalia postdates the critical episode of continental fragmentation, 148–110 Ma [27,48], questioning this hypothesis of vicariance driving placental mammal diversification.

A comprehensive divergence time study should account for three sources of uncertainty: the degree to which fossil calibrations approximate or encompass the time of divergence [25], the randomness in the molecular rate [22,36] and the variance of branch length estimates [49]. The variance in branch length estimates can be substantial for small sequence datasets leading to exceedingly large CIs for divergence times as has been observed in some studies [17]. These sources of uncertainty were not adequately addressed in molecular clock studies that supported particularly ancient dates of placental diversification [5,16]. Our Bayesian approach integrates genome-scale data with a conservative interpretation and realistic implementation of fossil-based time constraints [21], overcoming the limitations of previous analyses, and ameliorating this notorious instance of discord between molecular and palaeontological estimates of evolutionary time.

4. CONCLUSIONS

Palaeontologists have long understood that the first record of crown placentals in the early Paleogene is an underestimate of the age of Placentalia. Along with

other studies, we confirm that the explosive model, in which the last common ancestor of placentals postdates the K–Pg event, is incorrect. However, our results allow us to decisively reject a pre-extinction diversification, indicating instead the diversification of placental orders in a 20 Myr post-extinction interval. These results accord with the long fuse model [2] and are therefore consistent with the current interpretation of the mammalian fossil record. Our study is oriented around the genomic diversity of extant mammals. An important direction for future research concerns the extent to which the lack of genomic data from extinct groups, some of which were diverse shortly after the K–Pg boundary, may influence our ability to understand mammalian divergences generally. Nevertheless, we hypothesize that other instances of mismatch between molecular clocks and the fossil record, such as the origins of animal phyla, flowering plants, and modern birds, may be similarly reconciled without assuming extensive cryptic episodes of evolutionary history preceding their fossil records. Access to genome scale datasets through next generation sequencing makes realistic the prospect of an accurate and precise timescale for the Tree of Life.

REFERENCES

1 Benton, M. J. & Ayala, F. J. 2003 Dating the tree of life. *Science* **300**, 1698–1700. (doi:10.1126/science.1077795)
2 Archibald, J. D. & Deutschman, D. H. 2001 Quantitative analysis of the timing of the origin and diversification of extant placental orders. *J. Mamm. Evol.* **8**, 107–124. (doi:10.1023/A:1011317930838)
3 Alroy, J. 1999 The fossil record of north American mammals: evidence for a Paleocene evolutionary radiation. *Syst. Biol.* **48**, 107–118. (doi:10.1080/106351599260472)
4 Kemp, T. S. 2005 *The origin and evolution of mammals.* Oxford, UK: Oxford University Press.
5 Kumar, S. & Hedges, S. B. 1998 A molecular timescale for vertebrate evolution. *Nature* **392**, 917–920. (doi:10.1038/31927)
6 Cooper, A. & Fortey, R. 1998 Evolutionary explosions and the phylogenetic fuse. *Trends Ecol. Evol.* **13**, 151–156. (doi:10.1016/S0169-5347(97)01277-9)
7 Benton, M. J. 1999 Early origins of modern birds and mammals: molecules vs. morphology. *BioEssays* **21**,

1043–1051. (doi:10.1002/(SICI)1521-1878(199912) 22:1<1043::AID-BIES8>3E3.0.CO;2-B)

8 Foote, M., Hunter, J. P., Janis, C. M. & Sepkoski Jr, J. J. 1999 Evolutionary and preservational constraints on origins of biologic groups: divergence times of eutherian mammals. *Science* **283**, 1310–1314. (doi:10.1126/science.283.5406.1310)

9 Archibald, J. D., Averianov, A. O. & Ekdale, E. G. 2001 Late Cretaceous relatives of rabbits, rodents, and other extant eutherian mammals. *Nature* **414**, 62–64. (doi:10.1038/35102048)

10 Prasad, G. V. R., Verma, O., Sahni, A., Parmar, V. & Khosla, A. 2007 A Cretaceous hoofed mammal from India. *Science* **318**, 937. (doi:10.1126/science.1149267)

11 Asher, R. J., Meng, J., Wible, J. R., McKenna, M. C., Rougier, G. W., Dashzeveg, D. & Novacek, M. J. 2005 Stem lagomorpha and the antiquity of glires. *Science* **307**, 1091–1094. (doi:10.1126/science.1107808)

12 Wible, J. R., Rougier, G. W., Novacek, M. J. & Asher, R. J. 2009 The eutherian mammal *Maelestes gobiensis* from the late Cretaceous of Mongolia and the phylogeny of Cretaceous Eutheria. *Bull. Am. Museum Nat. Hist.* **327**, 1–123. (doi:10.1206/623.1)

13 Goswami, A., Prasad, G. V. R., Upchurch, P., Boyer, D. M., Seiffert, E. R., Verma, O., Gheerbrant, E. & Flynn, J. J. 2011 A radiation of arboreal basal eutherian mammals beginning in the late Cretaceous of India. *Proc. Natl Acad. Sci. USA* **108**, 16 333–16 338.(doi:10.1073/pnas.1108723108)

14 Hasegawa, M., Thorne, J. L. & Kishino, H. 2003 Time scale of eutherian evolution estimated without assuming a constant rate of molecular evolution. *Genes Genet. Syst.* **78**, 267–283. (doi:10.1266/ggs.78.267)

15 Springer, M. S., Murphy, W. J., Eizirik, E. & O'Brien, S. J. 2003 Placental mammal diversification and the Cretaceous–Tertiary boundary. *Proc. Natl Acad. Sci. USA* **100**, 1056–1061. (doi:10.1073/pnas.0334222100)

16 Bininda-Emonds, O. R. *et al.* 2007 The delayed rise of present-day mammals. *Nature* **446**, 507–512. (doi:10.1038/nature05634)

17 Meredith, R. W. *et al.* 2011 Impacts of the Cretaceous terrestrial revolution and K-Pg extinction on mammal diversification. *Science* **334**, 521–524. (doi:10.1126/science.1211028)

18 Kitazoe, Y., Kishino, H., Waddell, P. J., Nakajima, N., Okabayashi, T., Watabe, T. & Okuhara, Y. 2007 Robust time estimation reconciles views of the antiquity of placental mammals. *PLoS ONE* **2**, e384. (doi:10.1371/journal.pone.0000384)

19 Hallstrom, B. M. & Janke, A. 2010 Mammalian evolution may not be strictly bifurcating. *Mol. Biol. Evol.* **27**, 2804–2816. (doi:10.1093/molbev/msq166)

20 Hubbard, T. J. *et al.* 2009 ENSEMBL 2009 *Nucleic Acids Res.* **37**, D690–D697. (doi:10.1093/nar/gkn828)

21 Benton, M. J., Donoghue, P. C. J. & Asher, R. J. 2009 Calibrating and constraining molecular clocks. In *The timetree of life* (eds S. Blair Hedges & S. Kumar), pp. 35–86. Oxford, UK: Oxford University Press.

22 Rannala, B. & Yang, Z. 2007 Inferring speciation times under an episodic molecular clock. *Syst. Biol.* **56**, 453–466. (doi:10.1080/10635150701420643)

23 Guindon, S. 2010 Bayesian estimation of divergence times from large sequence alignments. *Mol. Biol. Evol.* **27**, 1768–1781. (doi:10.1093/molbev/msq060)

24 dos Reis, M. & Yang, Z. 2011 Approximate likelihood calculation on a phylogeny for Bayesian estimation of divergence times. *Mol. Biol. Evol.* **28**, 2161–2172. (doi:10.1093/molbev/msr045)

25 Yang, Z. & Rannala, B. 2006 Bayesian estimation of species divergence times under a molecular clock using multiple fossil calibrations with soft bounds. *Mol. Biol. Evol.* **23**, 212–226. (doi:10.1093/molbev/msj024)

26 Springer, M. S., Stanhope, M. J., Madsen, O. & de Jong, W. W. 2004 Molecules consolidate the placental mammal tree. *Trends Ecol. Evol.* **19**, 430–438. (doi:10.1016/j.tree.2004.05.006)

27 Nishihara, H., Maruyama, S. & Okada, N. 2009 Retroposon analysis and recent geological data suggest near-simultaneous divergence of the three superorders of mammals. *Proc. Natl Acad. Sci. USA* **106**, 5235–5240. (doi:10.1073/pnas.0809297106)

28 Loytynoja, A. & Goldman, N. 2008 Phylogeny-aware gap placement prevents errors in sequence alignment and evolutionary analysis. *Science* **320**, 1632–1635. (doi:10.1126/science.1158395)

29 Stamatakis, A., Ludwig, T. & Meier, H. 2005 RAxML-III: a fast program for maximum likelihood-based inference of large phylogenetic trees. *Bioinformatics* **21**, 456–463. (doi:10.1093/bioinformatics/bti191)

30 Janecka, J. E., Miller, W., Pringle, T. H., Wiens, F., Zitzmann, A., Helgen, K. M., Springer, M. S. & Murphy, W. J. 2007 Molecular and genomic data identify the closest living relative of Primates. *Science* **318**, 792–794. (doi:10.1126/science.1147555)

31 Hassanin, A. & Ropiquet, A. 2007 Resolving a zoological mystery: the kouprey is a real species. *Proc. R. Soc. B* **274**, 2849–2855. (doi:10.1098/rspb.2007.0830)

32 Sato, J. J., Wolsan, M., Minami, S., Hosoda, T., Sinaga, M. H., Hiyama, K., Yamaguchi, Y. & Suzuki, H. 2009 Deciphering and dating the red panda's ancestry and early adaptive radiation of Musteloidea. *Mol. Phylogenet. Evol.* **53**, 907–922. (doi:10.1016/j.ympev.2009.08.019)

33 Nilsson, M. A., Churakov, G., Sommer, M., Tran, N. V., Zemann, A., Brosius, J. & Schmitz, J. 2010 Tracking marsupial evolution using archaic genomic retroposon insertions. *PLoS Biol.* **8**, e1000436. (doi:10.1371/journal.pbio.1000436)

34 Eizirik, E., Murphy, W. J., Koepfli, K. P., Johnson, W. E., Dragoo, J. W., Wayne, R. K. & O'Brien, S. J. 2010 Pattern and timing of diversification of the mammalian order Carnivora inferred from multiple nuclear gene sequences. *Mol. Phylogenet. Evol.* **56**, 49–63. (doi:10.1016/j.ympev.2010.01.033)

35 Yang, Z. 2007 PAML 4: phylogenetic analysis by maximum likelihood. *Mol. Biol. Evol.* **24**, 1586–1591. (doi:10.1093/molbev/msm088)

36 Thorne, J. L., Kishino, H. & Painter, I. S. 1998 Estimating the rate of evolution of the rate of molecular evolution. *Mol. Biol. Evol.* **15**, 1647–1657. (doi:10.1093/oxfordjournals.molbev.a025892)

37 Hasegawa, M., Kishino, H. & Yano, T. 1985 Dating of the human-ape splitting by a molecular clock of mitochondrial DNA. *J. Mol. Evol.* **22**, 160–174. (doi:10.1007/BF02101694)

38 Yang, Z. 1994 Maximum likelihood phylogenetic estimation from DNA sequences with variable rates over sites: approximate methods. *J. Mol. Evol.* **39**, 306–314. (doi:10.1007/BF00160154)

39 Whelan, S. & Goldman, N. 2001 A general empirical model of protein evolution derived from multiple protein families using a maximum-likelihood approach. *Mol. Biol. Evol.* **18**, 691–699. (doi:10.1093/oxfordjournals.molbev.a003851)

40 Yang, Z., Nielsen, R. & Hasegawa, M. 1998 Models of amino acid substitution and applications to mitochondrial protein evolution. *Mol. Biol. Evol.* **15**, 1600–1611. (doi:10.1093/oxfordjournals.molbev.a025888)

41 Inoue, J., Donoghue, P. C. & Yang, Z. 2010 The impact of the representation of fossil calibrations on Bayesian

estimation of species divergence times. *Syst. Biol.* **59**, 74–89. (doi:10.1093/sysbio/syp078)

42 Kaufman, L. & Rousseeuw, P. J. 1990 *Finding groups in data: an introduction to cluster analysis.* New York, NY: John Wiley & Sons. (doi:10.1002/9780470316801)

43 Warnock, R. C. M., Yang, Z. & Donoghue, P. C. J. 2012 Exploring uncertainty in the calibration of the molecular clock. *Biol. Lett.* **8**, 156–159. (doi:10.1098/rsbl.2011.0710)

44 Luo, Z. X., Yuan, C. X., Meng, Q. J. & Ji, Q. 2011 A Jurassic eutherian mammal and divergence of marsupials and placentals. *Nature* **476**, 442–445. (doi:10.1038/nature10291)

45 Near, T. J. & Sanderson, M. J. 2004 Assessing the quality of molecular divergence time estimates by fossil calibrations and fossil–based model selection. *Phil. Trans. R. Soc. Lond. B* **359**, 1477–1483. (doi:10.1098/rstb.2004.1523)

46 Murphy, W. J., Pringle, T. H., Crider, T. A., Springer, M. S. & Miller, W. 2007 Using genomic data to unravel the root of the placental mammal phylogeny. *Genome Res.* **17**, 413–421. (doi:10.1101/gr.5918807)

47 Springer, M. S., Meredith, R. W., Janecka, J. E. & Murphy, W. J. 2011 The historical biogeography of mammalia. *Phil. Trans. R. Soc. B* **366**, 2478–2502. (doi:10.1098/rstb.2011.0023)

48 Schettino, A. & Turco, E. 2009 Breakup of Pangaea and plate kinematics of the Central Atlantic and Atlas regions. *Geophys. J. Int.* **178**, 1078–1097. (doi:10.1111/j.1365-246X.2009.04186.x)

49 Rodríguez-Trelles, F., Tarrío, R. & Ayala, F. J. 2002 A methodological bias toward overestimation of molecular evolutionary time scales. *Proc. Natl Acad. Sci. USA* **99**, 8112–8115. (doi:10.1073/pnas.122231299)

Supplementary Information

Bayesian estimation of divergence times

The objective of the Bayesian analysis is the estimation of the posterior probability, $f(\mathbf{t}, \mathbf{r}, \theta|D)$, of divergence times $\mathbf{t}$, molecular evolutionary rates $\mathbf{r}$, and model parameters θ, given the molecular data D. This posterior distribution is given by the Bayes theorem[1]

$$f(\mathbf{t}, \mathbf{r}, \theta|D) \propto f(\theta) f(\mathbf{t}) f(\mathbf{r}|\mathbf{t}, \theta) f(D|\mathbf{t}, \mathbf{r}, \theta) \tag{1}$$

where $f(\theta)$ is the prior of model parameters; $f(\mathbf{t})$ is the prior of times; $f(\mathbf{r}|\mathbf{t}, \theta)$ is the prior of rates on the tree; and $f(D|\mathbf{t}, \mathbf{r}, \theta)$ is the likelihood, or the probability of the molecular data given the times, rates, and model parameters. The posterior is generated by MCMC sampling.

In this study we faced two important challenges in using eq. (1). The first challenge was constructing the time prior,

$$f(\mathbf{t}) = f(\mathbf{t}_C) f_{BD}(\mathbf{t}_{\bar{C}}|\mathbf{t}_C), \tag{2}$$

which has two components: the density of ages for nodes in the tree for which fossil calibrations are available, $f(\mathbf{t}_C)$; and the conditional density, based on the birth and death (BD) process, for those nodes where no fossil calibrations are available, $f_{BD}(\mathbf{t}_{\bar{C}}|\mathbf{t}_C)$. The time prior must comply with the requirement that any node cannot be older than its ancestral nodes. During the MCMC iteration, node ages that violate this requirement are never proposed. Effectively $f(\mathbf{t}_C)$ is truncated, and the effective prior density used by the program may be very different from the user specified calibration density (e.g. node 40 in Supplementary Fig. 2). For this reason it is always necessary to examine the time prior, which can be easily generated by MCMC iteration without sequence data (that is, by setting $f(D|\mathbf{t}, \mathbf{r}, \theta) = 1$ in eq. 1).

We stress the importance of reporting the time prior in divergence time studies. For some data sets the truncation effect may be quite substantial[2]. Furthermore, not all Bayesian divergence time programs construct the time prior in the same manner, and reporting the time prior is essential for valid comparisons among different studies. In the program Beast[3], the time prior is generated not by a conditional construction as in eq. (2), but instead by a multiplicative construction that does not respect the rules of probability calculus[4]. The resulting effective prior may be in conflict with the user-specified fossil calibrations.

The second challenge was the likelihood function, which has to be calculated many times during the MCMC iteration. In this study we used an approximate method to calculate the likelihood[5]. This method saves computation time, and its accuracy has been extensively tested[6, 7]. However, the large number of partitions and the large number of species in this study still made the analysis computationally demanding. A typical MCMC run for the 14K data set and 20 partitions took ~20 days, and a typical MCMC run on the 274 species tree took 8 days. All the analyses of this study took over 874 processor days. The exact likelihood method, as is used in Beast[3], takes > 100 times more computation and would not have been feasible[7].

Supplementary Table 1 | Fossil calibrations used in this study.

|	Node	Minimum soft bound		Maximum soft bound	
37	Root	162.9	†*Amphitherium* (Theriimorpha)[8]	191.1	absence of theriimorphs from early Jurassic[8]
38	Theria	124	†*Eomaia* (Eutheria)[9]	171.2	absence of therians in mid-Jurassic[8]
39	Marsupialia	48.6	†*Djarthia* (Australidelphia)[10]	-	
40	Placentalia	–		131.5	†*Eomaia* (Eutherian) and †*Sinodelphys* (Metatheria)[8]
43	Paenungulata	55.6	†*Eritherium* (Proboscidea)[11]	-	
44	Xenarthra	55.6	†*Riostegotherium*[12]	-	
47	Eulipotyphla	61.5	†*Adunator* (Erinaceomorpha)[13]	-	
49	Cetartiodactyla	–		65.8	absence of crown artiodactyls in Paleocene[14]
	Cetacea	33.8	†*Llanocetus* (stem mysticete, calibration applied to the 274 species tree only)[15]	-	
51	Dolphin/Cow	52.4	†*Himalayacetus* (Cetacea)[14]	-	
53	Horse/ cat	62.5	†*Lambdotherium* (Perissodactyla)[16]	-	
54	Carnivora	39.68	†*Daphoenus* (Canifornia, Carnivora)[17]	65.8	absence of crown (but not stem, e.g., †*Protictis*) carnivorans in early Paleocene[17]
55	Chiroptera	48.6	†*Icaronycteris* (Chiroptera)[18]	-	
57	Glires	61.5	†*Heomys* (Rodentia)[19]	-	
58	Lagomorpha	48.6	Vastan calcanei (Leporidae, Lagomorpha)[20]	65.8	absence of crown lagomorphs in early Paleocene[21]
59	Rodentia	55.6	†*Sciuravus* (nested within crown Rodentia)[22]	65.8	absence of crown rodents in early Paleocene[21]
60	Guinea pig/ rat	52.5	†*Birbalomys* (stem Hystricognathi)[23]	58.9	absence of caviomorphs in late Paleocene[23]
61	Kangaroo rat/ rat	40.2	†*Ulkenulastomys* (Muridae)[24]	56.0	absence of crown rodents in Paleocene[25]
62	Muridae	10.4	†*Karnimata* (linage leading to *Rattus*)[26]	14.0	absence of crown murines in early Miocene[26]
63	Euarchonta	61.5	carpolestids and plesiadapids (extinct primate sister taxa)[27]	-	
64	Primates	55.6	†*Altiatlasius* (Euprimates)[28]	-	
65	Strepsirrhini	33.7	†*Karanisia* (Lorisiformes)[29]	55.6	absence of strepsirhines in Paleocene[29]
67	Anthropoidea	33.7	†*Catopithecus* (Catarrhini)[28]	-	
68	Catarrhini	23.5	†*Proconsul* (Hominoidea)[30]	34.0	absence of hominoids in late Eocene[28]
69	Hominidae	11.2	†*Sivapithecus* (Ponginae)[31]	33.7	absence of pongines in late Eocene[28]
70	Homininae	7.25	†*Chororapithecus* (stem-gorilla)[32]	-	
71	Hominini	5.7	†*Orrorin* (Hominini)[33]	10	absence of hominines in mid-Miocene[34]

Note on fossil calibrations: Choice of fossil calibrations followed Benton et al.[8], to which readers are referred for a more exhaustive discussion of fossil constraints in molecular clock studies. We added a soft minimum for Chiroptera based on early Eocene microchiropterans[18]. Also, contra Benton et al.[8], the oldest stem hystricognaths are early Eocene chapattimyids from Pakistan (e.g., *Birbalomys*[23]). Our calibrations were never used as hard constraints but served as the basis for probability distributions around which clock estimates were made. We assigned a minimum constraint based on reasonable consensus on the oldest occurrence of a member of a specific crown clade, as noted in the literature for each calibration in Supplementary Table 1. Maximum constraints were defined by the youngest occurrence of a well sampled interval which lacks the crown clade in question but yields members of one or more related but less-nested clades. For example, the late Eocene deposits of the Fayum lack any evidence of hominoids (i.e., catarrhines more closely related to apes than monkeys), despite a diverse record of anthropoid and some strepsirhine primates[28, 29]. For further discussion see Benton et al.[8]
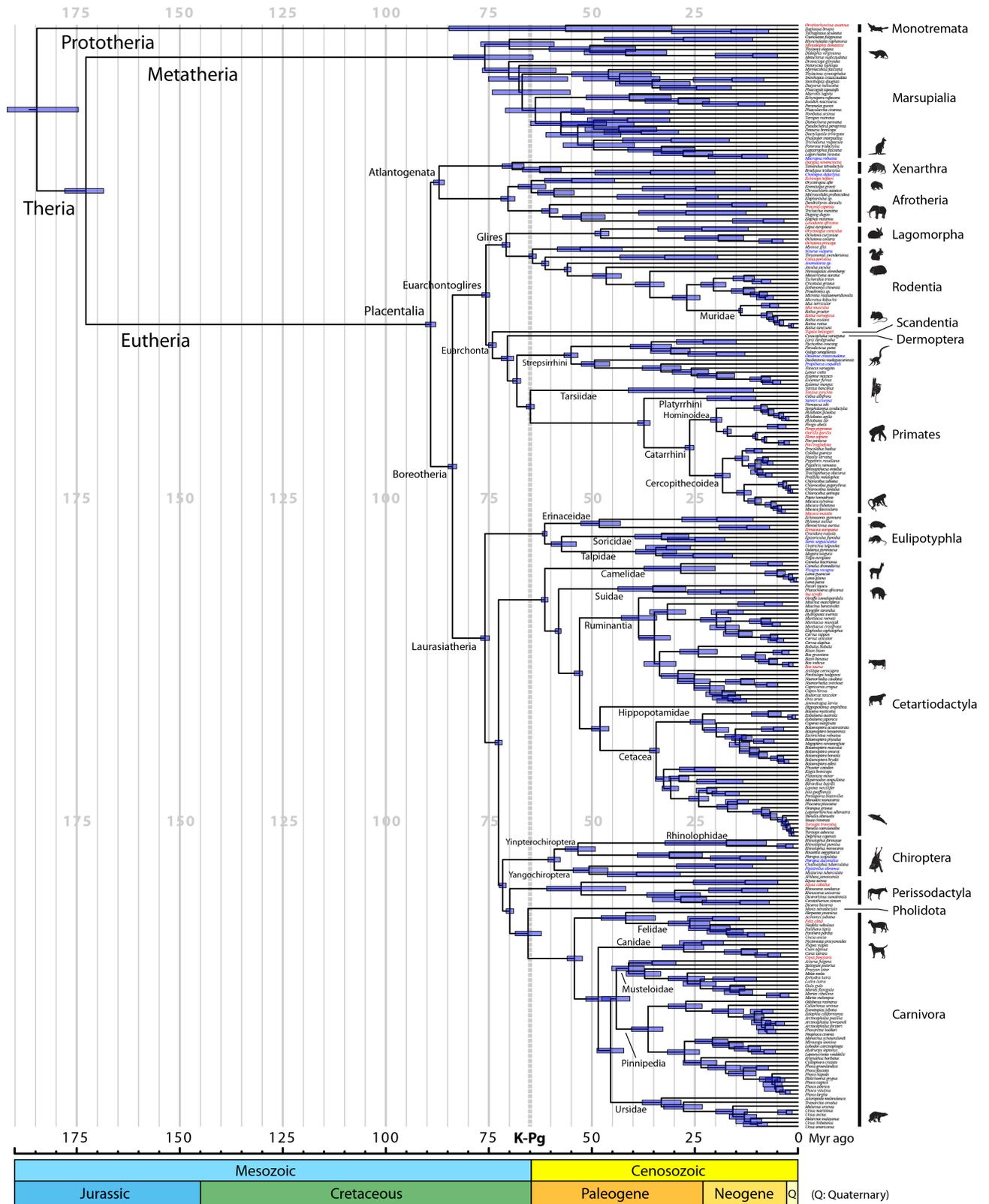
Supplementary Figure 1. The timetree of 274 mammal species. Blue bars represent the posterior 95% CI of node ages. Species for which nuclear genome data was analysed are shown in red. Species with nuclear genome data but without sequenced mitochondrial genomes were substituted by closely related species in the 274-species tree (indicated in blue). The tree was estimated by maximum likelihood using a guide tree incorporating well supported clades[35].

Times (Ma)
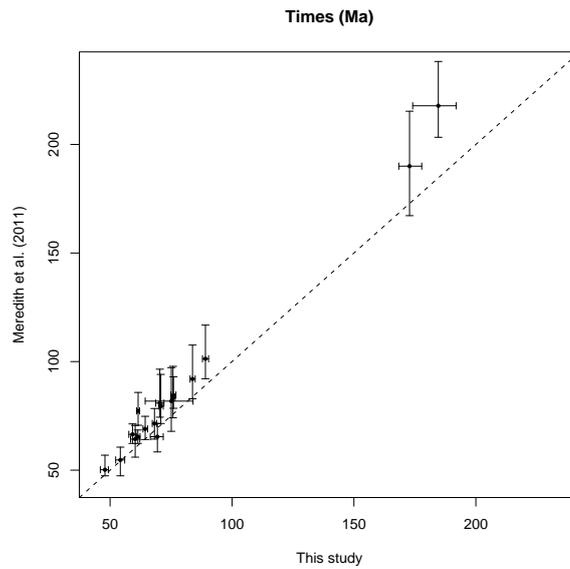
Supplementary Figure 2. Estimated divergence times in this study vs. the study of Meredith et al.[36] Vertical bars show the 95% CI in the study of Meredith et al.[36], and horizontal bars show the 95% CI in this study. Note the large uncertainty in Meredith et al.'s estimates.

Times (Ma)
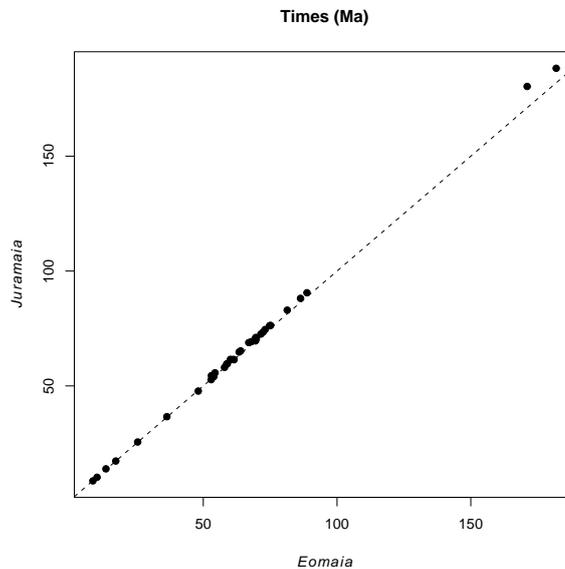
Supplementary Figure 3. Estimated divergence times using †*Eomaia* vs. †*Juramaia* calibrations. Divergence times were re-estimated on the 36 species tree (Atlantogenata topology) using the recently discovered †*Juramaia* fossil[37]. That is, the minimum calibration for node 38 was set to 149 Ma (Supplementary Table 1). The tail probability for the maximum bounds for nodes 37 and 38 was set to 0.1 (instead of the usual 0.025) to assess the effect of a more ancient root on estimated times. The rest of the calibrations were the same as in Supplementary Table 1.
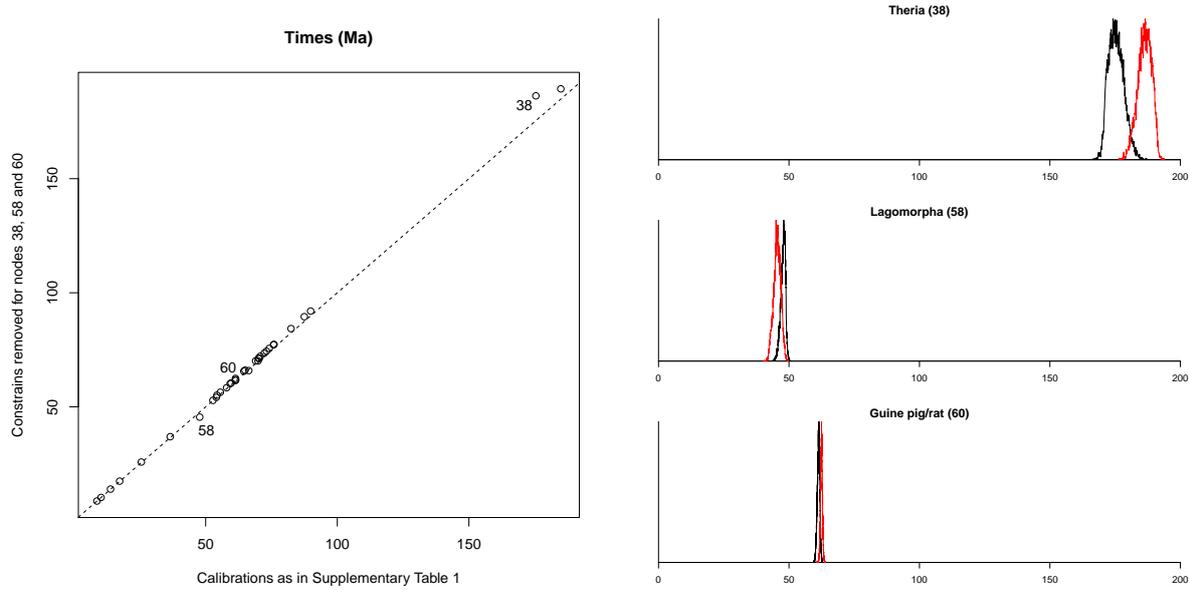
Supplementary Figure 4. Effect of conflicting fossil calibrations. Divergence times are estimated on the 36 species tree (Atlantogenata topology). A single analysis was carried out where the maximum age constraints of nodes 38 (Theria), 60 (Guinea pig/rat) and the joint constraints of node 58 (Lagomorpha) were removed because the original calibrations were in conflict with posterior time estimates (Fig. 3). Left panel: scatter plot of mean posterior ages calculated before (*x* axis) and after (*y* axis) removing the four constraints. Right panel: posterior time densities before (black lines) and after (red lines) removing the four constraints. After removing the constraints, the posterior age of node 38 became substantially older at 186 Ma (181-191), the posterior age of node 60 had little change at 62.5 Ma (61.7-63.2), and the posterior age of node 58 became slightly younger at 45.6 Ma (42.9-48.2). The posterior ages for the remaining nodes were marginally affected by the modified calibrations.
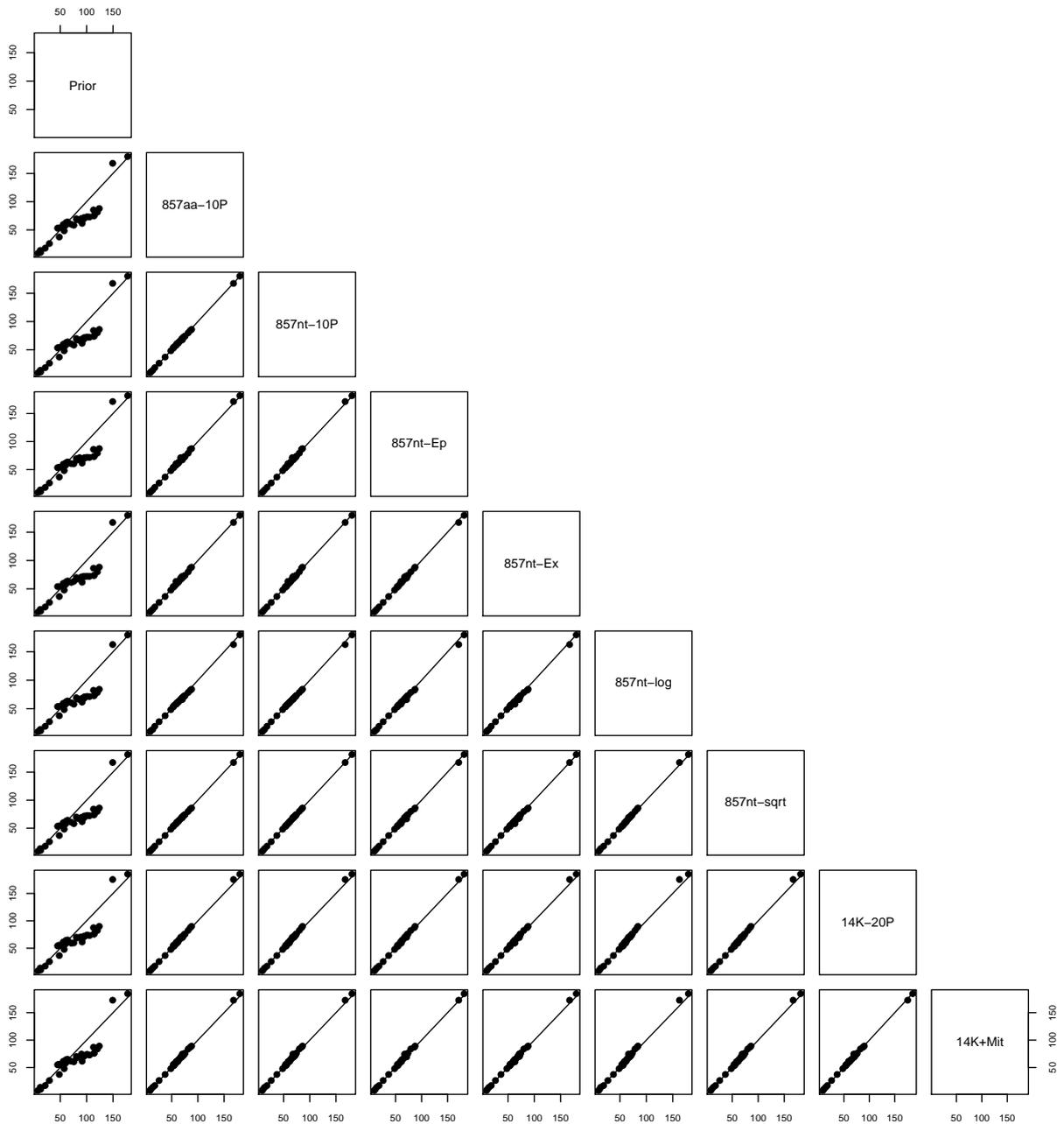
Supplementary Figure 5. Robustness of mean posterior time estimates. The molecular data are very informative and estimated times (in Myr) are very similar under various analysis conditions. 857aa-10P: 857 nuclear genes, amino acid substitution model, 10 partitions; 857nt-10P: 857 genes, nucleotide substitution model, 10 partitions; 857nt-Ep: nucleotide analysis, 10 partitions, with Epitheria placental topology; 857nt-Ex: nucleotide analysis, 10 partitions, with Exafroplacentalia placental topology; 857nt-log: 10 partitions generated by PCA of log-transformed branch lengths and k-means clustering of genes (see methods); 857nt-sqrt: 10 partitions generated by PCA of square root-transformed branch lengths and k-means clustering; 14K-20P: 14,632 nuclear genes, 20 partitions; and 14K+Mit: 12 mitochondrial proteins for 274 species, with prior constructed from the 14K-20P posterior times. Note that mean prior times are substantially older than mean posterior times for nodes dated $50 - 100$ Ma.

References

[1] Ziheng Yang. *Computational Molecular Evolution*. Oxford University Press, Oxford, 2006.

[2] J. Inoue, P. C. Donoghue, and Z. Yang. The impact of the representation of fossil calibrations on Bayesian estimation of species divergence times. *Syst Biol*, 59(1):74–89, 2010.

[3] A. J. Drummond and A. Rambaut. BEAST: Bayesian evolutionary analysis by sampling trees. *BMC Evol Biol*, 7:214, 2007.

[4] J. Heled and A.J. Drummond. Calibrated trees priors for relaxed phylogenetics and divergence time estimation. *Syst. Biol.*, in(the):press, 2011.

[5] J. L. Thorne, H. Kishino, and I. S. Painter. Estimating the rate of evolution of the rate of molecular evolution. *Mol Biol Evol*, 15(12):1647–57, 1998.

[6] M. dos Reis and Z. Yang. Approximate likelihood calculation on a phylogeny for Bayesian estimation of divergence times. *Mol Biol Evol*, 28(7):2161–72, 2011.

[7] F.U. Battistuzzi, P. Billing-Ross, A. Paliwal, and S. Kumar. Fast and slow implementations of relaxed clock methods show similar patterns of accuracy in estimating divergence times. *Mol Biol Evol*, 28(9):2439–2442, 2011.

[8] M.J. Benton, P.C.J. Donoghue, and R.J. Asher. *The Timetree of Life*, chapter Calibrating and constraining molecular clocks, pages 35–86. Oxford University Press, 2009.

[9] Q. Ji, Z.X. Luo, C.X. Yuan, J.R. Wible, J.P. Zhang, J.A. Georgi, et al. The earliest known eutherian mammal. *Nature*, 416(6883):816–822, 2002.

[10] R.M.D. Beck, H. Godthelp, V. Weisbecker, M. Archer, and S.J. Hand. Australia's oldest marsupial fossils and their biogeographical implications. *PLoS One*, 3(3):e1858, 2008.

[11] E. Gheerbrant. Paleocene emergence of elephant relatives and the rapid radiation of african ungulates. *Proc Natl Acad Sci USA*, 106(26):10717, 2009.

[12] L.P. Bergqvist, E.A. Abrantes, and L. dos Santos Avila. The xenarthra (mammalia) of são josé de itaboraí basin (upper paleocene, itaboraian), rio de janeiro, brazil. *Geodiversitas*, 26(2):323–337, 2004.

[13] M.C. McKenna, S.K. Bell, and G.G. Simpson. *Classification of Mammals above the Species Level*. Columbia Univ Press, 1997.

[14] S. Bajpai and P.D. Gingerich. A new eocene archaeocete (mammalia, cetacea) from india and the time of origin of whales. *Proc Nat Acad Sci USA*, 95(26):15464, 1998.

[15] E.M.G. Fitzgerald. The morphology and systematics of mammalodon colliveri (cetacea: Mysticeti), a toothed mysticete from the oligocene of australia. *Zool J Linn Soc*, 158(2):367–476, 2010.

[16] K.C. Beard. East of eden: Asia as an important center of taxonomic origination in mammalian evolution. *Bull Carnegie Mus Nat His*, 34:5–39, 1998.

[17] G.D. Wesley-Hunt and J.J. Flynn. Phylogeny of the carnivora: basal relationships among the carnivoramorphans, and assessment of the position of 'miacoidea' relative to carnivora. *J Syst Palaeontol*, 3(1):1–28, 2005.

[18] N.B. Simmons and J.H. Geisler. Phylogenetic relationships of icaronycteris, archaeonycteris, hassianycteris, and palaeochiropteryx to extant bat lineages, with comments on the evolution of echolocation and foraging strategies in microchiroptera. *Bull Am Mus Nat His*, 235:1–182, 1998.

[19] C.K. Li and S.Y. Ting. The paleogene mammals of china. *Bull Carnagie Mus Nat His*, 21:1–93, 1983.

[20] K.D. Rose, V.B. DeLeon, P. Missiaen, RS Rana, A. Sahni, L. Singh, and T. Smith. Early eocene lagomorph (mammalia) from western india and the early diversification of lagomorpha. *Proc Roy Soc B*, 275(1639):1203, 2008.

[21] R.J. Asher, J. Meng, J.R. Wible, M.C. McKenna, G.W. Rougier, D. Dashzeveg, and M.J. Novacek. Stem lagomorpha and the antiquity of glires. *Science*, 307(5712):1091, 2005.

[22] J. Meng, Y. Hu, and C. Li. The osteology of Rhombomylus (Mammalia, Glires): implications for phylogeny and evolution of Glires. *Bull Am Mus Nat His*, 275:1–247, 2003.

[23] L. Marivaux, M. Vianey-Liaud, and J.J. Jaeger. High-level phylogeny of early tertiary rodents: dental evidence. *Zool J Linn Soc*, 142(1):105–134, 2004.

[24] N.S. Shevyreva. *Flora i Fauna Zaysanskoi Vpadiny*, chapter New early Eocene rodents from the Zaysan Basin, pages 77–114. Akademiya Nauk Gruzinskoy SSR, Tblisi, 1984.

[25] J. Meng and A.R. Wyss. *The Rise of Placental Mammals: Origins and Relationships of the Major Extant Clades*, chapter Glires (Lagomorpha, Rodentia), pages 145–158. Johns Hopkins University Press, 2005.

[26] LL Jacobs and LJ Flynn. *Interpreting the Past: Essays on Human, Primate, and Mammal Evolution in Honor of David Pilbeam*, chapter Of mice ... again: the Siwalik rodent record, murine distribution, and molecular clocks, pages 63–80. Brill Academic Publishers, 2005.

[27] J.I. Bloch, M.T. Silcox, D.M. Boyer, and E.J. Sargis. New paleocene skeletons and the relationship of plesiadapiforms to crown-clade primates. *Proc Natl Acad Sci USA*, 104(4):1159, 2007.

[28] E.R. Seiffert, E.L. Simons, W.C. Clyde, J.B. Rossie, Y. Attia, T.M. Bown, P. Chatrath, and M.E. Mathison. Basal anthropoids from egypt and the antiquity of africa's higher primate radiation. *Science*, 310(5746):300, 2005.

[29] E.R. Seiffert, J.M.G. Perry, E.L. Simons, and D.M. Boyer. Convergent evolution of anthropoid-like adaptations in eocene adapiform primates. *Nature*, 461(7267):1118–1121, 2009.

[30] P. Tassy and M. Pickford. Un nouveau mastodonte zygolophodonte (proboscidea, mammalia) dans le miocčne inférieur d'afrique orientale: Systématique et paléoenvironnement. *Geobios*, 16(1):53–77, 1983.

[31] J. Kappelman, J. Kelley, D. Pilbeam, K.A. Sheikh, S. Ward, M. Anwar, J.C. Barry, B. Brown, P. Hake, N.M. Johnson, et al. The earliest occurrence ofsivapithecus from the middle miocene chinji formation of pakistan. *J Hum Evol*, 21(1):61–73, 1991.

[32] G. Suwa, R. T. Kono, S. Katoh, B. Asfaw, and Y. Beyene. A new species of great ape from the late Miocene epoch in Ethiopia. *Nature*, 448(7156):921–924, 2007.

[33] B.G. Richmond and W.L. Jungers. Orrorin tugenensis femoral morphology and the evolution of hominin bipedalism. *Science*, 319(5870):1662, 2008.

[34] D.R. Begun. Miocene hominids and the origins of the african apes and humans. *Ann Rev Anthropology*, 39:67–84, 2010.

[35] H. Nishihara, S. Maruyama, and N. Okada. Retroposon analysis and recent geological data suggest near-simultaneous divergence of the three superorders of mammals. *Proc Natl Acad Sci U S A*, 106(13):5235–40, 2009.

[36] R.W. Meredith, J.E. Janečka, J. Gatesy, O.A. Ryder, C.A. Fisher, E.C. Teeling, A. Goodbla, E. Eizirik, T.L.L. Simão, T. Stadler, et al. Impacts of the cretaceous terrestrial revolution and KPg extinction on mammal diversification. *Science*, 334(6055):521–524, 2011.

[37] Z.X. Luo, C.X. Yuan, Q.J. Meng, and Q. Ji. A Jurassic eutherian mammal and divergence of marsupials and placentals. *Nature*, 476(7361):442–445, 2011.